JOURNAL OF VIROLOGY, Sept. 2005, p. 11507–11512 Vol. 79, No. 17
0022-538X/05/$08.00+0 doi:10.1128/JVI.79.17.11507–11512.2005

Intracellular Localization of the Severe Acute Respiratory Syndrome Coronavirus Nucleocapsid Protein: Absence of Nucleolar Accumulation during Infection and after Expression as a Recombinant Protein in Vero Cells

Raymond R. R. Rowland,[1]* Vinita Chauhan,[1] Ying Fang,[2] Andrew Pekosz,[3] Maureen Kerrigan,[1] and Miriam D. Burton[4]

Diagnostic Medicine and Pathobiology, 1800 Denison Ave., Kansas State University, Manhattan, Kansas 66506[1]; Department of Veterinary Science, South Dakota State University, Brookings, South Dakota 57007[2]; Departments of Molecular Microbiology and Pathology & Immunology, Washington University School of Medicine, Campus Box 8230, 660 S. Euclid Ave., St. Louis, Missouri 63110[3]; and Department of Anatomy and Physiology, 1800 Denison Ave., Kansas State University, Manhattan, Kansas 66506[4]

Received 7 April 2005/Accepted 7 June 2005

The nucleocapsid (N) protein of several members within the order *Nidovirales* localizes to the nucleolus during infection and after transfection of cells with N genes. However, confocal microscopy of N protein localization in Vero cells infected with the severe acute respiratory syndrome coronavirus (SARS-CoV) or transfected with the SARS-CoV N gene failed to show the presence of N in the nucleoplasm or nucleolus. Amino acids 369 to 389, which contain putative nuclear localization signal (NLS) and nucleolar localization signal motifs, failed to restore nuclear localization to an NLS-minus mutant Rev protein. These data indicate that nuclear localization is not a conserved property among all nidoviruses.

Severe acute respiratory syndrome (SARS) is caused by an enveloped, positive-stranded RNA virus, the SARS coronavirus (SARS-CoV). Along with the arteriviruses, the coronaviruses are placed in a single order, *Nidovirales* (3). Even though nidovirus replication is restricted to the cytoplasm, the nucleocapsid proteins (N) of two arteriviruses, porcine reproductive and respiratory syndrome virus (PRRSV) and equine arteritis virus, have been reported to localize to the nucleolus during infection (19, 20, 23, 25). An identical cytoplasmic-nucleolar distribution pattern has also been reported for the N proteins of several coronaviruses, including representative members of group I (transmissible gastroenteritis virus [TGEV]), group II (mouse hepatitis virus [MHV]), and group III (infectious bronchitis virus [IBV]) viruses (11, 24). These arterivirus and coronavirus N proteins, when expressed alone or fused to the red-shifted enhanced green fluorescent protein (EGFP), also localize to the nucleolus, demonstrating that translocation across the nuclear pore complex and accumulation in the nucleolus are independent of other viral proteins (11, 20, 23). Once inside the nucleolus, the PRRSV and IBV N proteins colocalize with major nucleolar proteins, including nucleolin and fibrillarin (4, 25). The capacity of N to modulate nucleolar function may represent a viral strategy that diverts biosynthetic resources from the dividing nucleus to the cytoplasm, the site of virus replication (10, 11, 21, 25). There also appears to be a mechanism for the export of N from the nucleolus and back to the cytoplasm. The N proteins of PRRSV and equine arteritis virus accumulate in the nucleus in response to the treatment of cells with lemptomycin B (LMB) (20, 23), an inhibitor of the export shuttle protein CRM1 (7).

The classical scheme for the translocation of a protein from the cytoplasm through the nuclear pore complex and into the nucleoplasm is initiated through the interaction between a nuclear localization signal (NLS) on the cargo protein with the NLS-binding site on importin-α (reviewed in references 2 and 8). Classical NLS sequences are enriched in basic amino acids, such as lysines and arginines, and generally conform to one of three types, known as monopartite (pat4 and pat7) and bipartite motifs (9, 17). The pat4 NLS is defined as a continuous stretch of four basic amino acids (lysine or arginine) or three basic amino acids associated with histidine or proline. The pat7 NLS starts with proline followed within three residues by a segment containing three basic residues out of four. The "bipartite" motif consists of two basic amino acids, a 10-amino-acid spacer, and a 5-amino-acid segment containing at least three basic residues (reviewed in references 9 and 17). The nuclear transport of the PRRSV N protein is dependent on a single pat7 NLS, 41-PGKKNKK, which overlaps the RNA-binding domain (20, 22, 25). Site-directed scanning mutagenesis identified the requirement of the four lysine residues, 43-KK and 46-KK, for the transport of N into the nucleus (20). A second NLS, 10-KRKK, is located upstream and functions as a cryptic NLS which becomes accessible following a conformational change in the N protein (20, 21). The nucleolus is not a membrane-bound organelle; therefore, the localization of a protein to the nucleolus occurs by diffusion through the nucleoplasm and accumulation in the nucleolus via a *trans*-acting nucleolar targeting signal. Viral proteins frequently combine an NLS and nucleolar targeting signal into a single localization signal sequence, often referred to as a compact nucleolar localization signal (NoLS) sequence (14, 15). Compact NoLS

* Corresponding author. Mailing address: Diagnostic Medicine and Pathobiology, 1800 Denison Ave., Kansas State University, Manhattan, KS 66506. Phone: (785) 532-4631. Fax: (785) 532-4481. E-mail: browland@vet.ksu.edu.

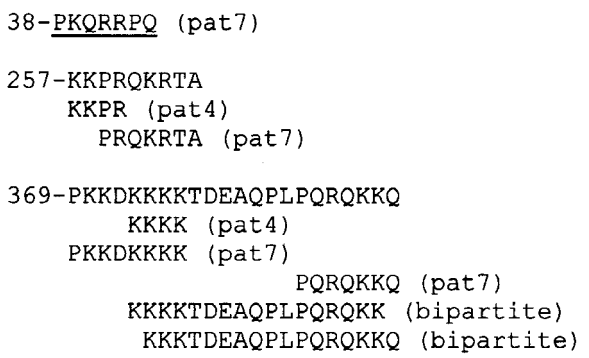

FIG. 1. NLS motifs in the SARS-CoV N protein. Peptide sequence analysis of the SARS-CoV N protein Urbani isolate (GenBank accession no. AY278741) was performed using the Web-based program PSORT (17). The rules for defining pat4, pat7, and bipartite motifs are discussed in the introductory comments of the text.

sequences are typically no longer than 30 amino acids and possess at least 9 basic amino acids, including at least one NLS motif (14).

When analyzed for the presence of NLS-like signal sequences using the computer program PSORT (17), the 422-amino-acid SARS-CoV N protein is shown to possess as many as eight NLS motifs, which are distributed between amino acids 38 to 44, 257 to 265, and 369 to 389 (Fig. 1). Embedded within the 369–389 domain are five NLS motifs, including a lysine-enriched peptide sequence, 369-PKKDKKK-375, which possesses similarities to the pat7 NLS in PRRSV N (20), and the well-characterized NLS, 126-PKKKRLV, found in the simian virus 40 large T antigen (13). In addition, the 369–375 region resembles the putative NLS sequence, 360-PKKEKKL, reported for the IBV N protein (24). The 369–389 region shares similarities with NoLS domains found in nucleolar proteins of other viral proteins, including human immunodeficiency virus Rev and Tat, human T-cell leukemia virus Rex, and the capsid protein of Semliki Forest virus (6, 14, 15, 21).

The localization of SARS-CoV N during infection was studied using confocal microscopy of infected cells stained with SA 46-4, a SARS-CoV N protein-specific monoclonal antibody (MAb) prepared in our laboratory against recombinant N prepared from the SARS-CoV Urbani isolate. Nuclei were identified using the nucleic acid stain TO-PRO-3 (Molecular Probes) (5). Vero cells (American Type Culture Collection) grown on coverslips were mock infected or infected with SARS-CoV (Urbani isolate) at a multiplicity of infection of 0.1. Coverslips were removed at 6, 12, and 24 h after infection, washed with phosphate-buffered saline (PBS), fixed for 10 min with 2% paraformaldehyde in PBS, and then stained with SA 46-4 followed by anti-mouse immunoglobulin G antibody conjugated to AlexaFluor 594 (Molecular Probes). All antibodies were diluted 1:500 in blocking buffer (PBS containing 3% normal goat sera and 0.2% saponin), and incubations were performed for 1 h at room temperature followed by extensive washing in PBS. Cells were counterstained with TO-PRO-3, diluted in blocking buffer, and then viewed on a Zeiss LSM 510 confocal microscope. In each experiment at least 50 infected cells in 10 distinct fields were analyzed. Representative results at 24 h after infection are presented in Fig. 2. A group of infected cells, presented in Fig. 2A, shows no evidence for anti-N staining in the nucleus or nucleolus. A higher magnification of a representative cell is presented in Fig. 2B, C, and D. We found no colocalization between SA 46-4 staining and the nuclear stain, TO-PRO-3. The same results were obtained from cells fixed and stained with SA 46-4 and TO-PRO-3 at 6 and 12 h after infection (data not shown).

Wurm et al. (24) reported the nucleolar localization of coronavirus N proteins in Vero cells transfected with N genes from TGEV, MHV, and IBV and stained with anti-N antibodies. IBV N tagged with EGFP also localized to the nucleolus of Vero cells (11). We performed similar studies of the SARS-CoV N gene expressed in Vero cells. A cDNA containing the N gene of SARS-CoV Urbani isolate was cloned into pIRES-EGFP, pEGFP-N1, and pEGFP-C2 eukaryotic expression vectors (Clontech). The pIRES-EGFP vector construct, pSARS-N-IRES-EGFP, through the incorporation of an internal ribosome entry site (IRES) separating the SARS-CoV N and EGFP genes, expresses EGFP and N as separate proteins. The other vectors express N as an EGFP fusion protein with the N protein fused in frame to the amino (SARS-N-EGFP) or carboxyl (EGFP-SARS-N) end of EGFP. The transfection of plasmid DNA into Vero cells was performed using Lipofectamine (Invitrogen) according to the manufacturer's directions. A representative cell at 24 h after transfection with pSARS-N-EGFP is shown in Fig. 3A, B, and C. Confocal microscopy showed that SARS-N-EGFP fluorescence was restricted to the cytoplasm with no visual evidence for N in the nucleolus. Similar results were obtained for Vero cells transfected with pSARS-N-IRES-EGFP and stained with the anti-N MAb SA 46-4 (data not shown). Hiscox et al. (11) reported only a small percentage of cells with IBV N protein in the nucleus/nucleolus. In cells transfected with pSARS-N-EGFP or pEGFP-SARS-N, we noticed that a small number of cells contained at least some EGFP fluorescence in the nucleoplasm, but not in the nucleoli. A single cell exhibiting EGFP fluorescence in the nucleus and stained with SA 46-4 is shown in Fig. 3D. The intensity of red (SA 46-4) and green (EGFP) fluorescence taken along a single axis through the cytoplasm and nucleus is presented in the profile below the photomicrograph. The fluorescence intensity profiles show that red fluorescence is primarily restricted to the cytoplasm (Fig. 3D), whereas EGFP fluorescence can be found in both nuclear and cytoplasmic compartments but is restricted from the nucleoli. The possibility that EGFP fluorescence in the nucleus was the result of free EGFP was confirmed by performing a Western blot assay of Vero cells transfected with pSARS-N-EGFP or pEGFP-SARS-N constructs. Proteins in cell lysates were separated by sodium dodecyl sulfate-polyacrylamide gel electrophoresis, transferred to a nylon membrane, and probed with anti-GFP antibody. The blot showed the presence of full-length N-EGFP and EGFP-N fusion proteins, as well as smaller-sized products, including immunoreactive proteins which migrated the same as free EGFP (data not shown). Therefore, the presence of EGFP in the nucleus of some transfected cells is likely the result of the proteolytic cleavage of the SARS-N-EGFP fusion protein and release of smaller-sized EGFP-labeled fragments. Collectively, the results from infected and transfected cells indicate that SARS-CoV N does not appear to target the nucleolus or nucleus.

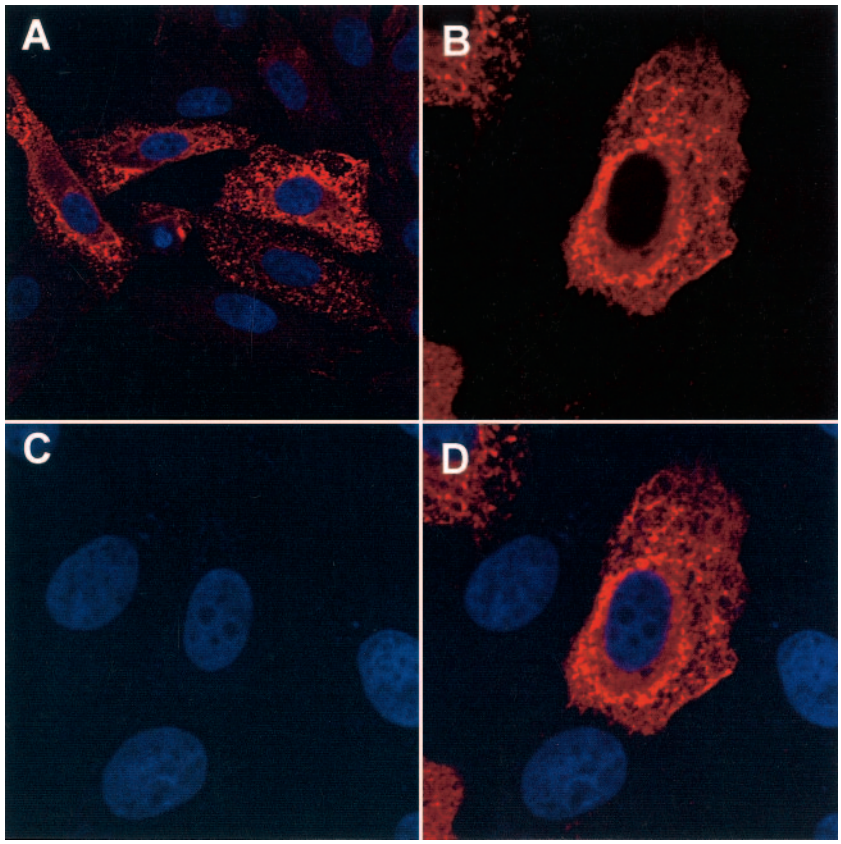

FIG. 2. Distribution of N in SARS-CoV-infected cells. (A) Confocal microscopy of a cluster of infected cells at 24 h after infection. Viral antigen was detected using AlexaFluor 594-labeled SA 46-4 anti-N MAb (red). Cells were counterstained with the nuclear stain TO-PRO-3 (blue). (B, C, and D) Images of a single representative infected cell at 24 h after infection. (B) AlexaFluor 594-labeled SA 46-4; (C) TO-PRO-3 staining; (D) merged image combining SA 46-4 and TO-PRO-3 staining. An 0.8-μm slice through the nucleus is shown in each image. Images were obtained with a 63× oil objective, and panels B, C, and D are magnified ×2.

One possible explanation for the absence of detectable amounts of N in the nucleus is that N enters the nucleus but is rapidly exported. Therefore, under steady-state conditions only a small quantity of N would be visible in the nucleus at any one time. In order to test this possibility, we treated pSARS-N-EGFP-transfected cells with the nuclear export blocker LMB, an antibiotic which inhibits CRM1, the major export shuttle protein (7, 18). LMB, at concentrations up to 50 nM, was added to Vero cells between 4 and 18 h after transfection. After addition of LMB, the live cells were then followed under a fluorescence microscope for an additional 24 h. Cells transfected with a recombinant equine infectious anemia virus Rev (ERev) cDNA fused to EGFP (pEGFP-ERev) were included as a positive control. The continuous shuttling of ERev back and forth between the cytoplasm and the nucleus is dependent on single NLS and nuclear export signal domains (16, 18). The majority of Vero cells transfected with pERev-EGFP showed the presence of ERev-EGFP fusion protein in the cytoplasm (Fig. 4A). In the presence of 10 nm LMB, the distribution pattern shifted towards the accumulation of ERev-EGFP in the nucleus (Fig. 4B). Accumulation of ERev-EGFP in the nucleus appeared as early as 6 h after the addition of LMB. Figure 4C and D show representative results for cells transfected with pSARS-N-EGFP and treated with LMB. The addition of LMB did not alter the cytoplasmic distribution of SARS-N-EGFP. The same result was obtained for cells transfected with pSARS-N-IRES-EGFP and stained with SA 46-4 (data not shown). LMB, when added as early as 4 h after transfection and at concentrations as high as 50 nM, did not affect the localization properties of SARS-N-EGFP. These data further support the notion that the SARS-CoV N protein is not translocated into the nucleus.

Putative NLS sequences in the N proteins of IBV, TGEV, and MHV coronaviruses are found at amino acids 340-RKRK, 391-PKPQRKR, and 360-PKKEKKL, respectively (11, 24). The corresponding region in SARS-CoV N protein is located in a lysine-rich region, between amino acids 369 and 389 (Fig. 1). Furthermore, the peptide sequence 369-PKKDKKK of SARS-CoV N is nearly identical to the well-characterized NLS in PRRSV N protein (20) as well as a putative NLS in the N protein of IBV (24). To determine if the 369–389 peptide possessed nuclear transport activity, we tested the ability of the 369–389 peptide to substitute for the NLS of ERev. The pat4 NLS of ERev was removed by deleting six amino acids, 159-K RRRKHL, from the C terminus. The construct, pERev(NLS-minus)N(369–389)EGFP, was made by ligating the cDNA corresponding to the SARS N 369–389 peptide to the C-terminal end of the mutant ERev and followed by EGFP. In Vero cells

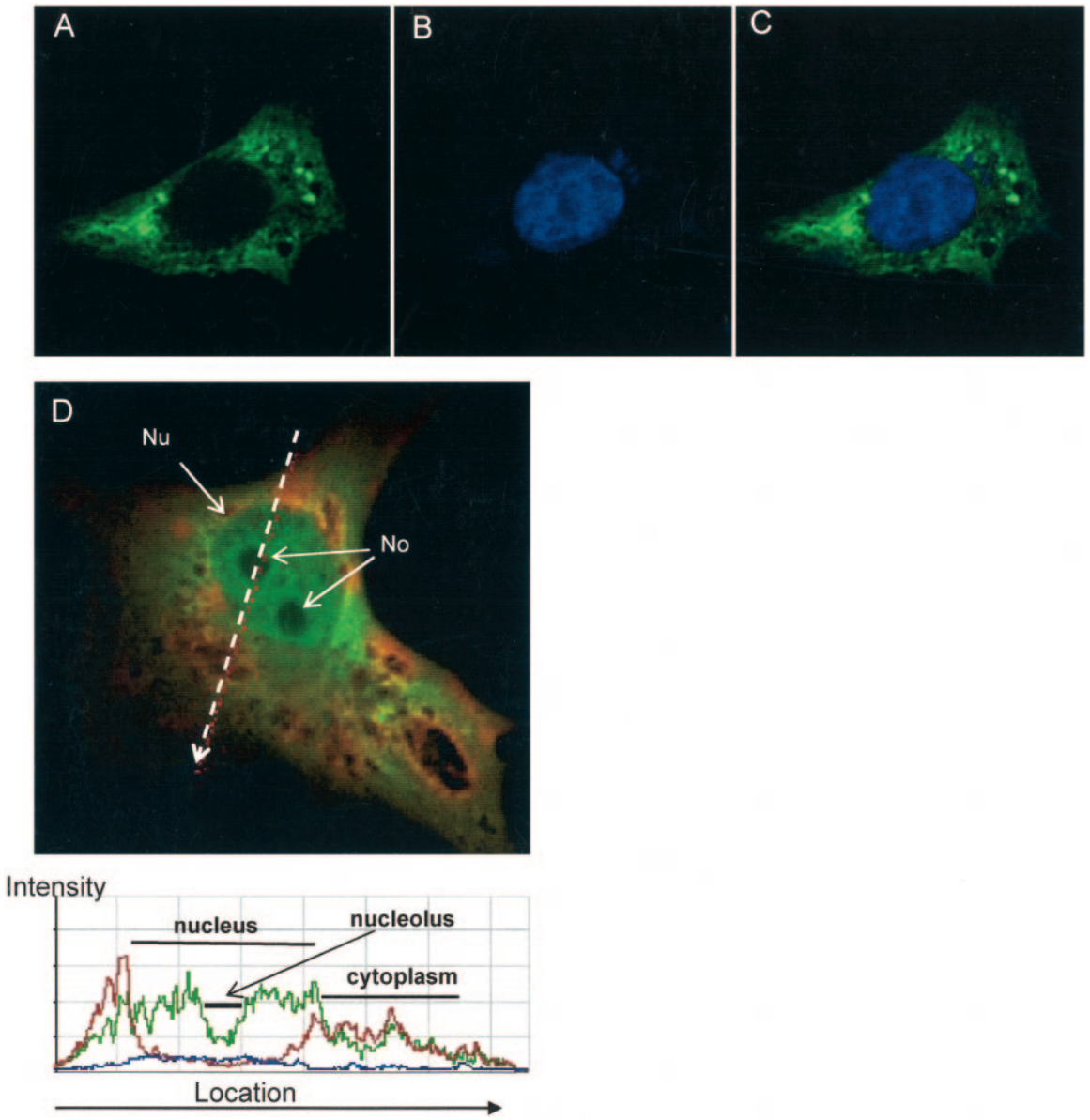

FIG. 3. Localization of SARS-CoV N-EGFP in Vero cells. (A, B, and C) Confocal microscopic images of a single cell at 24 h after transfection with pSARS-N-EGFP. (A) EGFP fluorescence; (B) TO-PRO-3 fluorescence; (C) merged image. (D) Image of a single cell transfected with pSARS-N-EGFP and exhibiting EGFP fluorescence in the nucleus. The cell was counterstained with AlexaFluor 594-labeled SA46-4 anti-N MAb (red). Below the image is a profile showing the intensity of EGFP (green line) and AlexaFluor 594 (red line) fluorescence along the axis shown by the dotted arrow in the image.

transfected with pERev(NLS-minus)N(369–389)EGFP, the chimeric EGFP protein localized to the cytoplasm (Fig. 4E). Blocking CRM1 by the addition of 10 nM LMB did not alter the cytoplasmic distribution of the chimeric protein (Fig. 4F). These data indicate that the 369–389 region of SARS-CoV N lacks the ability to substitute for the NLS of a known nucleocytoplasmic protein.

Presumably, the translocation of TGEV, MHV, and IBV coronavirus N proteins across the nuclear pore complex and into the nucleoplasm is dependent on the activities of classical NLS domains (11, 24). The presence of eight NLS motifs, scattered between three different regions of the SARS-CoV N polypeptide, provided a compelling argument for the nuclear and nucleolar localization of SARS-CoV N. However, the results from this study of N protein localization in Vero cells infected with SARS-CoV or transfected with constructs expressing the N gene showed no evidence for the localization of SARS-CoV N to the nucleoplasm or nucleolus. The absence of NLS activity within the lysine-rich 369–389 domain is puzzling. We can propose three mechanisms for the absence of NLS activity by the 369–389 peptide. First, even though NLS sequences frequently possess negatively charged residues, additional negative charges conferred by acidic amino acid residues or phosphorylated serine, threonine, or tyrosine residues can

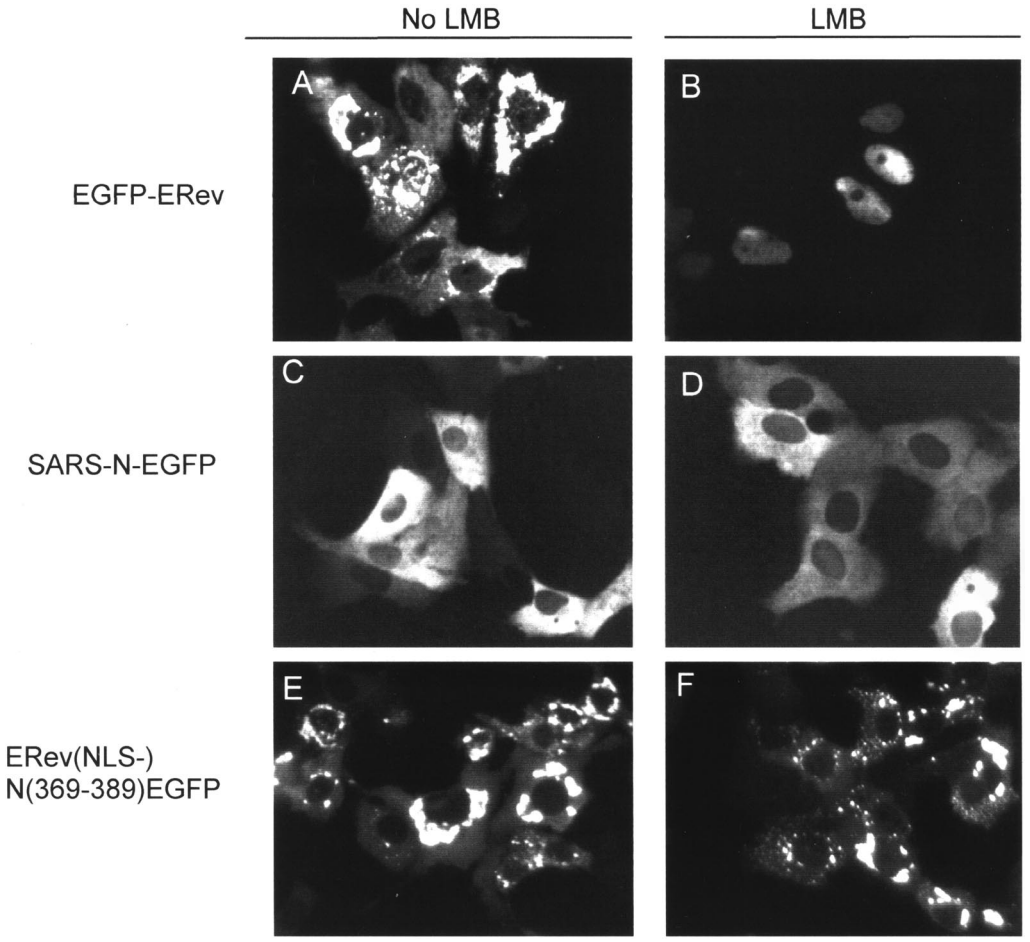

FIG. 4. Effect of LMB on localization of SARS-N-EGFP in live cells. (A and B) Cells transfected with the control construct, pEGFP-ERev. (C and D) Cells transfected with pSARS-N-EGFP. (E and F) Cells transfected with the Rev-SARS chimeric construct pRev(NLS-minus)SARS-N (368–389). LMB, at a concentration of 10 nM, was added at 4 h after transfection. The results following LMB treatment are shown in the panels on the right. Photomicrographs were taken at 18 h after transfection.

lower the affinity of the interaction between the NLS and NLS-binding site on importin-α (12). An aspartic acid residue is found at position 372, within the pat7 NLS motif of the SARS CoV-N. Additional, negatively charged amino acids are found at positions 378 and 379 (Fig. 1). One more negative charge is made available through the potential phosphorylation of threonine at position 377 (1). Therefore, four negatively charged residues may be sufficient to neutralize both monopartite and bipartite NLS sequences within the 369–389 region. A second possibility is that the NLS is in a poor conformation to be recognized by importin-α. And finally, NLS recognition may be sterically blocked by the interaction between the 369–389 region and a cytoplasmic protein. In this study we did not evaluate the nuclear localization properties of the NLS motifs located in the other regions of the SARS-CoV N protein. Since the SARS-CoV N protein does not appear to enter the nucleus, we can assume that these NLS motifs are inactive or inaccessible or that there are additional domains which are responsible for retaining N in the cytoplasm.

We acknowledge the assistance of Paul Rota and the Centers for Disease Control and Prevention for providing the SARS-CoV Urbani isolate and the SARS-CoV N gene cDNA. We are grateful to Susan Carpenter (Iowa State), who provided the cDNA of the ERev protein, and the Molecular Microbiology Imaging Facility (Washington University, St. Louis, Mo.).

This work was supported by National Institutes of Health grant U54 AI057160 to the Midwest Regional Center of Excellence for Biodefense and Emerging Infectious Diseases Research as well as by Department of Health and Human Services, Public Health Service grants P20 RR17708 to the University of Kansas COBRE program in Protein Structure and Function and AI059328 (A.P.).

REFERENCES

1. **Blom, N., S. Gammeltoft, and S. Brunak.** 1999. Sequence- and structure-based prediction of eukaryotic protein phosphorylation sites. J. Mol. Biol. **294:**1351–1362.
2. **Catimel, B., T. Teh, M. R. Fontes, I. G. Jennings, D. A. Jans, G. J. Howlett, E. C. Nice, and B. Kobe.** 2001. Biophysical characterization of interactions involving importin-alpha during nuclear import. J. Biol. Chem. **276:**34189–34198.
3. **Cavanagh, D.** 1997. Nidovirales: a new order comprising Coronaviridae and Arteriviridae. Arch. Virol. **142:**629–633.
4. **Chen, H., T. Wurm, P. Britton, G. Brooks, and J. A. Hiscox.** 2002. Interaction of the coronavirus nucleoprotein with nucleolar antigens and the host cell. J. Virol. **76:**5233–5250.
5. **De Maziere, A. M., W. J. Hage, and G. A. Ubbels.** 1996. A method for staining of cell nuclei in Xenopus laevis embryos with cyanine dyes for whole-mount confocal laser scanning microscopy. J. Histochem. Cytochem. **44:**399–402.

6. **Favre, D., E. Studer, and M. R. Michel.** 1994. Two nucleolar targeting signals present in the N-terminal part of Semliki Forest virus capsid protein. Arch. Virol. **137:**149–155.
7. **Fornerod, M., M. Ohno, M. Yoshida, and I. Mattaj.** 1997. CRM1 is an export receptor for leucine-rich nuclear export signals. Cell **90:**1051–1060.
8. **Gorlich, D., and U. Kutay.** 1999. Transport between the cell nucleus and the cytoplasm. Annu. Rev. Cell Dev. Biol. **5:**607–660.
9. **Hicks, G. R., and N. V. Raikhel.** 1995. Protein import into the nucleus: an integrated view. Annu. Rev. Cell Dev. Biol. **11:**155–188.
10. **Hiscox, J. A.** 2002. The nucleolus—a gateway to viral infection? Arch. Virol. **147:**1077–1089.
11. **Hiscox, J. A., T. Wurm, L. Wilson, P. Britton, D. Cavanagh, and G. Brooks.** 2001. The coronavirus infectious bronchitis virus nucleoprotein localizes to the nucleolus. J. Virol. **75:**506–512.
12. **Jans, D. A., and S. Hubner.** 1996. Regulation of protein transport to the nucleus: central role of phosphorylation. Physiol. Rev. **76:**651–685.
13. **Kalderon, D., B. L. Roberts, W. D. Richardson, and A. E. Smith.** 1984. A short amino acid sequence able to specify. Cell **39:**499–509.
14. **Kubota, S., T. D. Copeland, and R. J. Pomerantz.** 1999. Nuclear and nucleolar targeting of human ribosomal protein S25: common features shared with HIV-1 regulatory proteins. Oncogenes **18:**1503–1514.
15. **Kubota, S., H. Siomi, T. Satoh, S. Endo, M. Maki, and M. Hatanaka.** 1989. Functional similarity of HIV-I rev and HTLV-I rex proteins: identification of a new nucleolar targeting signal in rev protein. Biochem. Biophys. Res. Commun. **162:**963–970.
16. **Meyer, B. E., J. L. Meinkoth, and M. H. Malim.** 1996. Nuclear transport of human immunodeficiency virus type 1, visna virus, and equine infectious anemia virus Rev proteins: identification of a family of transferable nuclear export signals. J. Virol. **70:**2350–2359.
17. **Nakai, K., and M. Kanehisa.** 1992. A knowledge base for predicting protein localization sites in eukaryotic cells. Genomics **14:**897–911.
18. **Otero, G. C., M. E. Harris, J. E. Donello, and T. J. Hope.** 1998. Leptomycin B inhibits equine infectious anemia virus Rev and feline immunodeficiency virus rev function but not the function of the hepatitis B virus posttranscriptional regulatory element. J. Virol. **72:**7593–7597.
19. **Rowland, R. R., R. Kervin, C. Kuckleburg, A. Sperlich, and D. A. Benfield.** 1999. The localization of porcine reproductive and respiratory syndrome virus nucleocapsid protein to the nucleolus of infected cells and identification of a potential nucleolar localization signal sequence. Virus Res. **64:**1–12.
20. **Rowland, R. R., P. Schneider, Y. Fang, W. Wootton, D. Yoo, and D. A. Benfield.** 2003. Peptide domains involved in the localization of the porcine reproductive and respiratory syndrome virus nucleocapsid protein to the nucleolus. Virology **16:**135–145.
21. **Rowland, R. R., and D. Yoo.** 2003. Nucleolar-cytoplasmic shuttling of PRRSV nucleocapsid protein: a simple case of molecular mimicry or the complex regulation by nuclear import, nucleolar localization and nuclear export signal sequences. Viral Res. **95:**23–33.
22. **Siomi, H., H. Shida, S. H. Nam, T. Nosaka, M. Maki, and M. Hantanaka.** 1988. Sequence requirements for nucleolar localization of human T-cell leukemia virus type I pX proteins, which regulates viral RNA processing. Cell **55:**197–209.
23. **Tijms, M. A., Y. van der Meer, and E. J. Snijder.** 2002. Nuclear localization of non-structural protein 1 and nucleocapsid protein of equine arteritis virus. J. Gen. Virol. **83:**795–800.
24. **Wurm, T., H. Chen, T. Hodgson, P. Britton, G. Brooks, and J. A. Hiscox.** 2001. Localization to the nucleolus is a common feature of coronavirus nucleoproteins, and the protein may disrupt host cell division. J. Virol. **75:**9345–9356.
25. **Yoo, D., S. K. Wootton, G. Li, C. Song, and R. R. Rowland.** 2003. Colocalization and interaction of the porcine arterivirus nucleocapsid protein with the small nucleolar RNA-associated protein fibrillarin. J. Virol. **77:**12173–12183.